Int. J. Solids Structures, 1969, Vol. 5, pp. 491 to 511. Pergamon Press. Printed in Great Britain

THE EFFECT OF COUPLE-STRESSES ON THE DIFFRACTION OF PLANE ELASTIC WAVES BY CYLINDRICAL DISCONTINUITIES

H. R. AGGARWAL and R. C. ALVERSON

Stanford Research Institute, Menlo Park, California

Abstract—This investigation considers the effect of couple-stresses on dynamical stresses developed around a circular cylindrical discontinuity embedded in an infinite medium by the diffraction of steady plane parallel elastic compressional waves propagating in the medium. Both a cavity and a rigid cylinder with an immovable cylinder treated as a special case of the latter are considered. Numerical results valid at large wavelengths for a fixed Poisson's ratio showing variation of the modified stresses against different parameter ratios involved are presented in the form of curves and compared with their classical values obtained as a limiting case. In either case, at certain wavelengths, quite appreciable deviations from classical results occur. The effect of couple-stresses on the motion of a rigid cylinder is discussed.

1. INTRODUCTION

THE linearized couple-stress theory has become an active field of research in recent years. This theory takes into account couple-stresses and rotation gradients neglected in classical infinitesimal elasticity theory. For centro-symmetric isotropic materials, consideration of these effects requires the introduction of two new material constants. One of these constants can be expressed as a length parameter presumably representing a size effect of the material. Thus, in problems wherein a small geometric dimension is associated with a stressed body, stress analysis according to the modified theory becomes highly desirable.

The influence of couple-stresses on static stress concentrations occurring around discontinuities and at crack tips has been examined in some recent studies. Few dynamic cases have been investigated. The purpose of the present investigation is to examine the effect of couple-stresses on dynamic stress concentrations. The problem treated here concerns a steady plane elastic compressional wave propagating in an infinite couple-stress medium and diffracted by a circular cylindrical discontinuity embedded in the medium with its axis parallel to the wavefront. The computed results showing the effects of the material characteristic length l may be used together with experiments to test the importance or relevance of the theory in appropriate materials.

The couple-stress dynamic plane strain theory in terms of displacement potentials is developed first from the three dimensional vector equations derived by Mindlin and Tiersten [1] and is subsequently employed in the study of the problem. Both a cavity and a rigid cylinder with an immovable cylinder treated as a special case of the latter are studied. Because of the vast involved analyses associated with the problem, the present work is limited to the part dealing only with finite frequencies.

The study shows that the modified stresses, in addition to their dependence on the parameters reported in the studies neglecting couple-stresses, also depend on the ratio of the radius of the discontinuity to the material characteristic length. Results for a fixed Poisson's ratio showing variation of these stresses against different parameter ratios involved are presented in the form of curves and compared against their classical values

obtained as a limiting case. In either case, at certain wavelengths, quite appreciable deviations from the classical results occur. The results show that the modified dynamic factors for a cavity, unlike their static counterpart, may, depending upon the incident wavelength, be greater or smaller than their corresponding classical dynamic values. In the case of a rigid cylinder the modified dynamic factors, for the range of wave numbers considered, are always greater than their corresponding classical dynamic factors. For Poisson's ratio 0·25 and radius-material characteristic length ratio 3, the modified dynamic factors for a cavity at nondimensional wave numbers (2π radius/wave length) 0·25 and 4 are, respectively, 13·4 per cent less and 17·3 per cent greater than the corresponding classical dynamic values. In the case of rigid cylinder, the modified dynamic factor for the stated parameters and nondimensional wave number 1·5 is, for different densities of the cylinder, about 27 to 28 per cent larger than its classical dynamic value. To contrast the dynamic deviations against the static ones, the static modified factors at the given parameters in case of uniaxial strain are 12·4 per cent less for a cavity and 16 per cent greater for a rigid cylinder than their corresponding classical static values. The effect of couple-stresses on the motion of a rigid cylinder is also discussed.

2. DYNAMIC PLANE STRAIN EQUATIONS: COUPLE-STRESS THEORY

The basic three-dimensional equations governing the motion of centrosymmetric-isotropic homogeneous materials in the linearized couple-stress theory are derived in [1]. The corresponding plane strain equations are obtained by appropriately restricting the three-dimensional equations to two dimensions. The displacement potential form of the plane strain theory in general curvilinear coordinates will be stated here. Its derivation, without any loss of generality, assumes the first invariant of the couple-stress tensor to be constant, a condition necessary for a continuous transition of the linearized couple-stress to the classical elasticity theory [2].

Let θ_α, $\alpha = 1, 2$, represent a system of curvilinear coordinates in the plane of no strain taken as $\theta_3(= z) = 0$ and $\mathbf{k}$ be the unit vector along the normal to this plane. The Stokes–Helmholtz displacement potentials appropriate to the plane strain case may be taken as $\varphi(\theta_1, \theta_2)$ and $\Psi(\theta_1, \theta_2)\mathbf{k}$, and the associated set of governing equations are given as

Displacement vector

$$u_\alpha = \varphi_{,\alpha} - \varepsilon^{\beta\gamma} g_{\alpha\gamma} \Psi_{,\beta}, \qquad u_3 = 0. \tag{1}$$

Rotation vector

$$\omega_3 = -\tfrac{1}{2}\nabla^2 \Psi, \qquad \omega_\alpha = 0. \tag{2}$$

Force–stress tensor

$$\begin{aligned}
\tau_{\alpha\beta} &= \tau_{(\alpha\beta)} + \tau_{[\alpha\beta]}, \\
\tau_{(\alpha\beta)} &= \lambda g_{\alpha\beta} \nabla^2 \varphi + \mu[2\varphi_{,\alpha\beta} + \varepsilon^{\gamma\delta}(g_{\beta\gamma}\Psi_{,\alpha\delta} + g_{\alpha\gamma}\Psi_{,\beta\delta})], \\
\tau_{(\beta\alpha)} &= \tau_{(\alpha\beta)}, \\
\tau_{[\alpha\beta]} &= \eta \varepsilon_{\alpha\beta} \nabla^4 \Psi, \qquad \tau_{[\beta\alpha]} = -\tau_{[\alpha\beta]}, \\
\tau_{33} &= \lambda \nabla^2 \varphi, \qquad \tau_{\alpha 3} = \tau_{3\alpha} = 0.
\end{aligned} \tag{3}$$

Couple-stress tensor

$$\mu_{\alpha 3} = 2\eta(\nabla^2\Psi),\alpha, \qquad \mu_{3\alpha} = \nu^*\mu_{\alpha 3},$$
$$\mu_{11} = \mu_{22} = \mu_{33} = \text{constant}, \qquad \mu_{12} = \mu_{21} = 0. \tag{4}$$

Equations of motion

In the absence of body forces and body couples, the equations of motion may be taken as

$$c_1^2\nabla^2\varphi = \ddot{\varphi}, \qquad c_2^2(1-l^2\nabla^2)\nabla^2\Psi = \ddot{\Psi}. \tag{5}$$

As noted in [1], equations (1) and (5) comprise the complete solution to the corresponding displacement equations of motion.

In the above, the usual surface tensor notation [3] is followed with the exception that a comma preceded by a subscript denotes covariant derivative with regard to that variable, $\varepsilon^{\alpha\beta}$ is the contravariant skew-symmetric tensor of order 2, $g_{\alpha\beta}$ is the covariant metric tensor and ∇^2 is the Laplacian of the curvilinear system, $\nabla^4 = \nabla^2\nabla^2$, λ and μ are the Lamé's constants, η is the material constant resisting curvature-twist, ν^* is a non-dimensional number having a character similar to that of the Poisson's ratio, l is the material characteristic length defined by $\eta = \mu l^2$, c_1 and c_2 are, respectively, the dilatational and shear wave velocities, and $\dot{(\,)} = \partial/\partial t$, t being the time.

Boundary conditions

If n^α denotes the unit outward normal at a regular point of the bounding curve in a $\theta_1-\theta_2$ plane of the body, then the boundary conditions [1, p. 434] reduce† to in the specification of one factor in each of the three products:

$$(n^1\tau_{11}+n^2\tau_{21})u^1, \qquad (n^1\tau_{12}+n^2\tau_{22})u^2, \qquad (n^1\mu_{13}+n^2\mu_{23})\omega^3. \tag{6}$$

For a subsequent use equations involving covariant differentiations will be rewritten for the two special systems of rectangular cartesian and plane polar coordinates. The other equations in any system are readily written in terms of physical components by employing the Laplacian and the skew-symmetric tensor belonging to the system.

Rectangular Cartesian Coordinates: $\theta_1 = x$, $\theta_2 = y$.

$$u_x = \frac{\partial\varphi}{\partial x}+\frac{\partial\Psi}{\partial y}, \qquad u_y = \frac{\partial\varphi}{\partial y}-\frac{\partial\Psi}{\partial x}. \tag{7}$$

$$\tau_{xx} = \lambda\nabla^2\varphi+2\mu\left[\frac{\partial^2\varphi}{\partial x^2}+\frac{\partial^2\Psi}{\partial x\partial y}\right],$$
$$\tau_{xx}+\tau_{yy} = 2(\lambda+\mu)\nabla^2\varphi, \tag{8}$$
$$\tau_{(xy)} = \mu\left[2\frac{\partial^2\varphi}{\partial x\partial y}-\frac{\partial^2\Psi}{\partial x^2}+\frac{\partial^2\Psi}{\partial y^2}\right].$$

$$\mu_{xz} = -2\eta\frac{\partial}{\partial x}(\nabla^2\Psi), \qquad \mu_{yz} = -2\eta\frac{\partial}{\partial y}(\nabla^2\Psi). \tag{9}$$

Plane Polar Coordinates: $\theta_1 = r$, $\theta_2 = \theta$.

† Products (6) easily follow by noting that the scalar μ_{nn} in [1] in the plane strain case is a constant thus permitting equation (5.16) in [1] giving $\mathbf{p}$ to be written as $\mathbf{p} = (\mathbf{n}\,.\,\tau)$.

$$u_r = \frac{\partial \varphi}{\partial r} + \frac{1}{r}\frac{\partial \Psi}{\partial \theta}, \qquad u_\theta = \frac{1}{r}\frac{\partial \varphi}{\partial \theta} - \frac{\partial \Psi}{\partial r}. \tag{10}$$

$$\tau_{rr} = \lambda \nabla^2 \varphi + 2\mu\left[\frac{\partial^2 \varphi}{\partial r^2} - \frac{1}{r^2}\frac{\partial \Psi}{\partial \theta} + \frac{1}{r}\frac{\partial^2 \Psi}{\partial r \partial \theta}\right],$$

$$\tau_{rr} + \tau_{\theta\theta} = 2(\lambda + \mu)\nabla^2 \varphi, \tag{11}$$

$$\tau_{(r\theta)} = \mu\left[\frac{2}{r}\frac{\partial^2 \varphi}{\partial r \partial \theta} - \frac{2}{r^2}\frac{\partial \varphi}{\partial \theta} - \frac{\partial^2 \Psi}{\partial r^2} + \frac{1}{r}\frac{\partial \Psi}{\partial r} + \frac{1}{r^2}\frac{\partial^2 \Psi}{\partial \theta^2}\right].$$

$$\mu_{rz} = -2\eta \frac{\partial}{\partial r}(\nabla^2 \Psi), \qquad \mu_{\theta z} = -\frac{2\eta}{r}\frac{\partial}{\partial \theta}(\nabla^2 \Psi). \tag{12}$$

Before stating the problem, a remark on wave motion in an infinite, couple-stress medium† is in order. Wave analysis of potential equations (5) shows that three kinds of waves may propagate in the medium: an irrotational wave propagating non-dispersively with dilatational wave velocity as in a medium without couple-stresses and two dispersive transverse shear waves, one propagating and the other non-propagating.

3. PROBLEM

A plane time-harmonic compressional stress wave propagating in an infinite couple-stress medium interacts on an infinitely long parallel circular cylindrical discontinuity embedded in the medium, Fig. 1. It is desired to determine the stresses produced at the

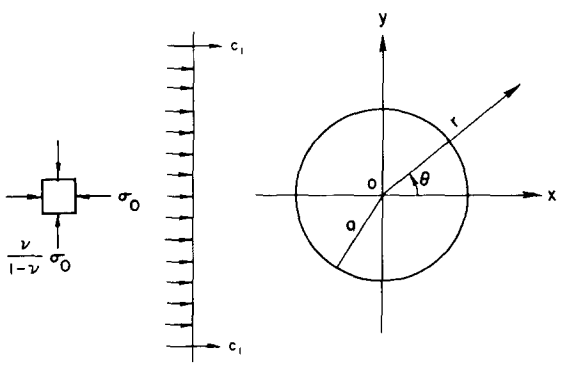

FIG. 1. Problem and coordinates.

surface of the discontinuity by the structure–medium interaction.‡ The problem is one of plane strain and constitutes the dynamic analog of the problems considered in [5, 6, 7] when the field at infinity is that of a uniaxial strain.

As the incident wave impinges on the discontinuity, according to the remark above, an irrotational and two shear waves are generated and scattered into the medium. The

† A couple-stress medium from here on will be taken to mean a linear centrosymmetric-isotropic homogeneous couple-stress medium.

‡ A corresponding problem for the case of a spherical cavity was considered recently in [4].

total field thus consists of two fields, the incident field and the scattered field, and is obtained by superposing the two. If the potentials (φ^I, Ψ^I) and (φ^s, Ψ^s), respectively, represent the incident and the scattered fields, then the potentials (φ, Ψ) representing the total field are

$$\varphi = \varphi^I + \varphi^s, \qquad \Psi = \Psi^I + \Psi^s. \tag{13}$$

The incident potentials are easily determined from the description of the incident wave and the potential equations (5). The potentials for the scattered field are obtained by solving equations (5) by the usual method of separation of variables and applying appropriate boundary conditions at the surface of the discontinuity and the radiation conditions at infinity. The infinite series representation thus obtained for the scattered potentials is apt for the description of finite frequency interaction response in regions near the discontinuity. The appropriate form of the solution suited to the study of very high frequency—very short wavelength—near or far field approximations may be obtained from the series solution by the use of Poisson's summation formula [8] or Watson's transformation [9]. An entire investigation of the scattered field, because of the vast involved analyses associated with it, would rather be an ambitious task. Accordingly, the present study is confined to finite frequencies. To further simplify the analysis, only the cases of a circular cavity and a rigid circular cylinder are considered.

The incident potentials, by equations (5) and the first of equations (8) and the geometry shown in Fig. 1, are found to be

$$\varphi^I = \varphi_0 \, e^{i(\alpha x - \omega t)}, \qquad \Psi^I = 0, \tag{14}$$

where $\varphi_0 = -\sigma_0/(\rho\omega^2)$, σ_0 is the stress-amplitude of the incoming wave, ω is the circular frequency, and α is the wave number defined by $\alpha = \omega/c_1 = 2\pi/\lambda$, λ being the wavelength.

Assuming both φ^s and Ψ^s to exhibit harmonic time-dependence one may write

$$\varphi^s = \bar{\varphi}^s \, e^{-i\omega t}, \qquad \Psi^s = \bar{\Psi}^s \, e^{-i\omega t}. \tag{15}$$

By equations (5), $\bar{\varphi}^s$ and $\bar{\Psi}^s$ are solutions of

$$(\nabla^2 + \alpha^2)\bar{\varphi}^s = 0, \qquad (\nabla^2 + \beta_1^2)(\nabla^2 - \beta_2^2)\bar{\Psi}^s = 0, \tag{16}$$

where

$$\begin{aligned} 2l^2\beta_j^2 &= (1 + 4l^2\beta^2)^{\frac{1}{2}} + (-1)^j, \qquad j = 1, 2, \\ \beta^2 &= \omega^2/c_2^2. \end{aligned} \tag{17}$$

As noted in [1], the complete solution of (16) can be expressed as

$$\bar{\Psi}^s = \bar{\Psi}^s_1 + \bar{\Psi}^s_2, \tag{18}$$

where $\bar{\Psi}^s_1$ and $\bar{\Psi}^s_2$ are governed by Helmholtz' equations

$$(\nabla^2 + \beta_1^2)\bar{\Psi}^s_1 = 0, \qquad (\nabla^2 - \beta_2^2)\bar{\Psi}^s_2 = 0. \tag{19}$$

If the center of the discontinuity is taken at the origin of the polar coordinates, Fig. 1, the potentials $\bar{\varphi}^s$, $\bar{\Psi}^s_1$ and $\bar{\Psi}^s_2$, by the first of equations (16) and equation (19), meeting the symmetry conditions about the initial line $\theta = 0$ and the radiation conditions at infinity

(outgoing waves with diminishing amplitudes) may be written

$$\begin{aligned}\bar{\varphi}^s &= \varphi_0 \sum_{n=0}^{\infty} A_n H_n(\alpha r)\cos n\theta,\\ \bar{\Psi}_1^s &= \varphi_0 \sum_{n=0}^{\infty} B_n H_n(\beta_1 r)\sin n\theta,\\ \bar{\Psi}_2^s &= \varphi_0 \sum_{n=0}^{\infty} C_n K_n(\beta_2 r)\sin n\theta,\end{aligned} \tag{20}$$

where H_n is the Hankel function of the first kind of order n (the usual superscript (1) dropped for convenience), K_n is the modified Bessel function of the second kind, and A_n, B_n and C_n are constants to be determined from the boundary conditions at the discontinuity surface $r = a$, a being the radius of the discontinuity. One may, for convenience in algebraic manipulations, write φ^I also in series form [10]† as

$$\varphi^I = \varphi_0 \sum_{n=0}^{\infty} \varepsilon_n i^n J_n(\alpha r)\cos n\theta\, e^{-i\omega t}, \tag{21}$$

where J_n is the Bessel function of the first kind of order n, and ε_n is the Neumann's factor defined as

$$\varepsilon_0 = 1, \qquad \varepsilon_n = 2, \qquad n \geq 1. \tag{22}$$

Equations (13), (14), (15), (18), (20) and (21) together lead to a series representation of potentials φ and Ψ. Any pertinent field quantities may be derived by substituting the series expressions for φ and Ψ in the appropriate member(s) of the set of equations (2), (3), (4), (10), (11) and (12).

4. THE SOLUTIONS

Cavity

The boundary conditions in case of a traction free cavity, consistent with products (6), are

$$\tau_{rr} = \tau_{r\theta} = \mu_{rz} = 0, \qquad r = a. \tag{23}$$

Application of these boundary conditions gives the unknown constants in equations (20) as

$$\begin{aligned}A_n &= \varepsilon_n i^n [2i(L_n/M_n) - J_n(\alpha a)]/H_n(\alpha a),\\ B_n &= n\varepsilon_n i^{n-1}(\beta^2 a^2 - 2n^2 + 2)/[M_n H_n(\beta_1 a)],\\ C_n &= B_n N_n H_n(\beta_1 a)/K_n(\beta_2 a),\end{aligned} \tag{24}$$

† Item No. 94.

where

$$\begin{aligned}
L_n &= (\beta^2a^2/2-n+n^3)(1+N_n)-(n^2-1)[h_n(\beta_1a)-N_nk_n(\beta_2a)],\\
M_n &= \pi H_n(\alpha a)\Delta_n,\\
N_n &= \gamma^2[n-h_n(\beta_1a)]/[n+k_n(\beta_2a)], \qquad \gamma^2 = \beta_1^2/\beta_2^2,\\
\Delta_n &= (\beta^2a^2/4)(\beta^2a^2-4n-4n^2)(1+N_n)\\
&\quad +(\beta^2a^2/2-n+n^3)[h_n(\beta_1a)-N_nk_n(\beta_2a)]+h_n(\alpha a)L_n,
\end{aligned} \tag{25}$$

$h_n(z)$ and $k_n(z)$ are the quotient functions, defined by

$$h_n(z) = zH_{n-1}(z)/H_n(z), \qquad k_n(z) = zK_{n-1}(z)/K_n(z), \tag{26}$$

and use is made of the recurrence relations [10]

$$\begin{aligned}
zH_n'(z) &= -nH_n(z)+zH_{n-1}(z),\\
zK_n'(z) &= -nK_n(z)-zK_{n-1}(z),
\end{aligned} \tag{27}$$

and of the Wronskian

$$J_n(z)H_{n-1}(z)-J_{n-1}(z)H_n(z) = 2i/(\pi z). \tag{28}$$

The non-zero stresses at the cavity surface, from equations (11), (12) and (3) aided by equations (5) and (19) and the boundary conditions (23), are obtained as

$$\begin{aligned}
\tau_{\theta\theta|r=a} &= 4\sigma_0(1-1/k^2)\sum_{n=0}^{\infty}\varepsilon_n i^{n+1}(L_n/M_n)\cos n\theta\, e^{-i\omega t},\\
\tau_{\theta r|r=a} &= \frac{4\sigma_0}{\beta^2}\sum_{n=1}^{\infty}\frac{ni^{n-1}(\beta^2a^2-2n^2+2)}{M_n}[\beta^2(1+N_n)-\beta_1^2X_n]\sin n\theta\, e^{-i\omega t},\\
\mu_{\theta z|r=a} &= -4\sigma_0(l^2\beta_1^2/a\beta^2)\sum_{n=1}^{\infty}n^2i^{n-1}(\beta^2a^2-2n^2+2)(X_n/M_n)\cos n\theta\, e^{i\omega t},
\end{aligned} \tag{29}$$

where

$$k^2 = \beta^2/\alpha^2 = c_1^2/c_2^2 = 2(1-\nu)/(1-2\nu), \tag{30}$$

ν being the Poisson's ratio,

$$\begin{aligned}
X_n &= Y_n/[n+k_n(\beta_2a)],\\
Y_n &= h_n(\beta_1a)+k_n(\beta_2a).
\end{aligned} \tag{31}$$

From† the asymptotic expansions of the Bessel functions $H_n(z)$ and $K_n(z)$ for a fixed z and large n [10, item nos. 132 and 205], it is seen that the series asymptotic to the infinite series in equations (29) converge absolutely and uniformly by the ratio test for finite nondimensional wave numbers αa (and therefore for finite frequencies). A comparison test further applied to the latter series establishes their absolute and uniform convergence at finite αa. The non-suitability of the solution at very large frequencies is easily seen from the fact that no asymptotic expansion uniformly valid for all large n is available.

† The remarks here apply equally to all infinite series to appear subsequently.

The corresponding results in the special cases of the classical dynamic theory and the static theories with and without the couple-stresses may be obtained from equations (29) through limiting processes:

$$\lim_{\substack{l \to 0 \\ \omega \text{ fixed}}} \text{(dynamic couple-stress case)} \to \text{dynamic classical case},$$

$$\lim_{\substack{\omega \to 0 \\ l \text{ fixed}}} \text{(dynamic couple-stress case)} \to \text{static couple-stress case},$$

or

$$\left.\begin{matrix} \lim_{\omega \to 0} \text{(dynamic classical case)} \\ \lim_{l \to 0} \text{(static couple-stress case)} \end{matrix}\right\} \to \text{static classical case.}$$

The results in these special cases are as follows:

Dynamic case classical theory

$$\begin{aligned} \tau_{\theta\theta|r=a} &= 4\sigma_0(1-1/k^2)\sum_{n=0}^{\infty} \varepsilon_n i^{n+1}(L_n^0/M_n^0)\cos n\theta\, e^{-i\omega t}, \\ \tau_{\theta r|r=a} &= \mu_{\theta z|r=a} = 0, \end{aligned} \tag{32}$$

where

$$\begin{aligned} L_n^0 &= \beta^2 a^2/2 - n + n^3 - (n^2-1)h_n(\beta a), \\ M_n^0 &= \pi H_n(\alpha a)\Delta_n^0, \\ \Delta_n^0 &= (\beta^2 a^2/4)(\beta^2 a^2 - 4n - 4n^2) + (\beta^2 a^2/2 - n + n^3)h_n(\beta a) + h_n(\alpha a)L_n^0. \end{aligned} \tag{33}$$

The plane stress version of this case was previously studied by Pao [11] and equations (32) agree with his results after necessary modifications.

Static case couple-stress theory

$$\begin{aligned} \tau_{\theta\theta|r=a} &= \frac{\sigma_0}{1-\nu}\left[1 - \frac{2(1-2\nu)}{1+F_1}\cos 2\theta\right], \\ \tau_{\theta r|r=a} &= -\frac{2\sigma_0[2+k_1(a/l)]F_1 \sin 2\theta}{k^2(1+F_1)}, \\ \mu_{\theta z|r=a} &= \frac{2a\sigma_0 F_1 \cos 2\theta}{k^2(1+F_1)}, \end{aligned} \tag{34}$$

where

$$F_1 = \frac{8(1-\nu)}{4+(a/l)^2+2k_1(a/l)}. \tag{35}$$

Static case classical theory

$$\begin{aligned} \tau_{\theta\theta|r=a} &= \frac{\sigma_0}{1-\nu}[1 - 2(1 \mp 2\nu)\cos 2\theta], \\ \tau_{\theta r|r=a} &= \mu_{\theta z|r=a} = 0. \end{aligned} \tag{36}$$

Equations (34) and (36) agree, respectively, with the results for the uniaxial strain case obtained from [5] and [12].

Equations (32), (34) and (36) utilize the following approximations:

For $\beta^2 l^2 \to 0$,

$$\beta_1^2 = \beta^2[1+0(l^2\beta^2)], \qquad \beta_2^2 = \frac{1}{l^2}[1+0(l^2\beta^2)],$$
$$\gamma^2 = \beta^2 l^2[1+0(l^2\beta^2)]. \tag{37}$$

For $z \to 0$, z real (see [10]),

$$H_0(z) = \frac{2i}{\pi}\ln z + 0(1), \qquad H_1(z) = -\frac{2i}{\pi z} + 0(z \ln z),$$
$$H_n(z) = -i\frac{(n-1)!}{\pi}\left(\frac{2}{z}\right)^n[1+0(z^2)], \qquad n \geq 2,$$
$$h_0(z) = \frac{1}{\ln z}[1+0(1/\ln z)], \qquad h_1(z) = -z^2[\ln z + 0(1)], \tag{38}$$
$$h_2(z) = \frac{z^2}{2}[1+0(z^2 \ln z)], \qquad h_n(z) = \frac{z^2}{2(n-1)}[1+0(z^2)], \qquad n \geq 3.$$

For $z \to \infty$, z real (see [10]),

$$k_n(z) = z[1+0(1/z)], \qquad n \geq 0. \tag{39}$$

Rigid cylinder. Finite density

The boundary conditions for a rigid cylinder of finite density ρ_c, consistent with products (6) are

$$u_r = U\cos\theta, \qquad u_\theta = -U\sin\theta, \qquad \omega_z = 0, \qquad r = a, \tag{40}$$†

where U is the x-displacement of the cylinder. The quantity U is determined from the force–balance equation

$$M\ddot{U} = \int_0^{2\pi} (\tau_{rr}\cos\theta - \tau_{r\theta}\sin\theta)_{r=a} a\, d\theta, \tag{41}$$

where M is mass per unit-length of the cylinder. In view of the third of the boundary conditions above and the periodicity of the circular functions $\sin n\theta$ the equation for the rate of change of angular momentum

$$I\ddot{\omega}_z = \int_0^{2\pi} (a\tau_{r\theta} + \mu_{rz})_{r=a} a\, d\theta,$$

where I is the axial moment of inertia of the cylinder, is automatically satisfied.

† From symmetry of the problem, there is no vertical motion and no rigid-body rotation about its axis of the cylinder.

Application of these boundary conditions gives the unknown constants appearing in equations (20) and the displacement U as

$$\left.\begin{aligned} A_0 &= -J_1(\alpha a)/H_1(\alpha a).\\ A_1 &= -2i[J_1(\alpha a)+2ix/m]/H_1(\alpha a),\\ B_1 &= 4(s-1)/[mH_1(\beta_1 a)],\\ A_n &= -2i^n[J_n(\alpha a)+2ix_n/m_n]/H_n'(\alpha a),\\ B_n &= 4ni^{n-1}/[m_n H_n(\beta_1 a)],\\ C_n &= B_n\gamma^2 H_n(\beta_1 a)/K_n(\beta_2 a), \end{aligned}\right\} \quad n \geq 2, \tag{42}$$

$$U = \frac{\varphi_0}{as}[2iJ_1(\alpha a)+A_1 H_1(\alpha a)+B_1(1+\gamma^2)H_1(\beta_1 a)], \tag{43}$$

where

$$\left.\begin{aligned} x &= (s+1)(1+\gamma^2)+s\gamma^2 k_1(\beta_2 a)-sh_1(\beta_1 a), \qquad s = \rho_c/\rho,\\ m &= \pi H_1(\alpha a)\delta,\\ x_n &= n(1+\gamma^2)+\gamma^2 k_n(\beta_2 a)-h_n(\beta_1 a),\\ m_n &= \pi H_n(\alpha a)\delta_n,\\ \delta &= (1/s)[\{s+1-sh_1(\alpha a)\}x-(s-1)^2(1+\gamma^2)],\\ \delta_n &= [n-h_n(\alpha a)]x_n-n^2(1+\gamma^2), \end{aligned}\right\} \tag{44}$$

and use is made of the recurrence relations (27) and the Wronskian (28). The stresses at the surface of the cylinder, from equations (11), (12), and (3) together with the use of equations (5) and (19), are obtained as

$$\left.\begin{aligned} \tau_{rr|r=a} &= 2\sigma_0\left[\frac{i^{-1}}{\pi\alpha a H_1(\alpha a)}+\frac{2x\cos\theta}{m}+2\sum_{n=2}^{\infty}\frac{i^{n-1}x_n}{m_n}\cos n\theta\right]e^{-i\omega t},\\ \tau_{\theta\theta|r=a} &= (1-2/k^2)\tau_{rr|r=a},\\ \tau_{r\theta|r=a} &= -4\sigma_0(1+\gamma^2)\left[\frac{(s-1)}{m}\sin\theta+\sum_{n=2}^{\infty}\frac{ni^{n-1}}{m_n}\sin n\theta\right]e^{-i\omega t},\\ \mu_{rz|r=a} &= -\frac{8\sigma_0 l^2}{a}\left(\frac{\beta_1}{\beta}\right)^2\left[\frac{(s-1)Y_1\sin\theta}{m}+\sum_{n=2}^{\infty}\frac{ni^{n-1}Y_n}{m_n}\sin n\theta\right]e^{-i\omega t}, \end{aligned}\right\} \tag{45}$$

and

$$\mu_{\theta z|r=a} = 0.$$

For the special cases described earlier, the pertinent limiting processes aided by approximations (37–39) give

Dynamic case classical theory

$$\begin{aligned}
\tau_{rr}|_{r=a} &= 2\sigma_0[1/\{i\pi\alpha a H_1(\alpha a)\} + (2/m^0)\{s+1-sh_1(\beta a)\}\cos\theta \\
&\quad + 2\sum_{n=2}^{\infty}(i^{n-1}/m_n^0)\{n-h_n(\beta a)\}\cos n\theta]\,e^{-i\omega t}, \\
\tau_{\theta\theta}|_{r=a} &= (1-2/k^2)\tau_{rr}|_{r=a}, \\
\tau_{r\theta}|_{r=a} &= -4\sigma_0[(1/m^0)(s-1)\sin\theta + \sum_{n=2}^{\infty}(ni^{n-1}/m_n^0)\sin n\theta]\,e^{-i\omega t}, \\
\mu_{rz}|_{r=a} &= 0,
\end{aligned} \tag{46}$$

where

$$\begin{aligned}
m^0 &= \pi H_1(\alpha a)\delta^0, \qquad m_n = \pi H_n(\alpha a)\delta_n^0, \\
\delta^0 &= 4-(s+1)[h_1(\alpha a)+h_1(\beta a)]+sh_1(\alpha a)h_1(\beta a), \\
\delta_n^0 &= -nh_n(\alpha a)-nh_n(\beta a)+h_n(\alpha a)h_n(\beta a).
\end{aligned} \tag{47}$$

The plane stress analog of this case was previously considered by Pao and Mow [13].

Static case couple-stress theory

$$\begin{aligned}
\tau_{rr|r=a} &= \sigma_0\left[1+\frac{2(1-2\nu)\cos 2\theta}{3-4\nu-F_2}\right], \\
\tau_{\theta\theta|r=a} &= (1-2/k^2)\tau_{rr|r=a}, \\
\tau_{r\theta|r=a} &= -\frac{2\sigma_0(1-2\nu)}{3-4\nu-F_2}\sin 2\theta, \\
\mu_{rz|r=a} &= -\frac{2\sigma_0 aF_2}{k^2[3-4\nu-F_2]}\sin 2\theta,
\end{aligned} \tag{48}$$

where

$$F_2 = \frac{4(1-\nu)}{2+k_1(a/l)}. \tag{49}$$

Equations (48) are in agreement with the corresponding results deduced from [7].

Static case classical theory

$$\begin{aligned}
\tau_{rr|r=a} &= \sigma_0\left[1+\frac{2(1-2\nu)}{3-4\nu}\cos 2\theta\right], \qquad \tau_{\theta\theta|r=a} = (1-2/k^2)\tau_{rr|r=a}, \\
\tau_{r\theta|r=a} &= -\frac{2\sigma_0(1-2\nu)}{3-4\nu}\sin 2\theta, \qquad \mu_{rz|r=a} = 0
\end{aligned} \tag{50}$$

which agree with the stress field for the uniaxial strain case derived from [12].

In either static case, the real part of the displacement of the cylinder is zero (see Appendix) and as a consequence the boundary conditions (40) reduce to their usual form employed in static studies [6, 7, 12].

Rigid cylinder. Infinite density

The stresses developed at the cylindrical surface of an infinitely dense rigid cylinder may be obtained from those for a finitely dense cylinder through the limiting process letting the density ratio s go to infinity. This gives:

Dynamic case couple-stress theory

$$\begin{aligned}
\tau_{rr|r=a} &= 2\sigma_0 \sum_{n=0}^{\infty} \varepsilon_n i^{n-1}(x_n/m_n)\cos n\theta\, e^{-i\omega t},\\
\tau_{\theta\theta|r=a} &= (1-2/k^2)\tau_{rr|r=a},\\
\tau_{r\theta|r=a} &= -4\sigma_0(1+\gamma^2) \sum_{n=1}^{\infty} (ni^{n-1}/m_n)\sin n\theta\, e^{-i\omega t},\\
\mu_{rz|r=a} &= -8\sigma_0(l^2\beta_1^2/a\beta^2) \sum_{n=1}^{\infty} ni^{n-1}(Y_n/m_n)\sin n\theta\, e^{-i\omega t}.
\end{aligned} \tag{51}$$

Dynamic case classical theory

$$\begin{aligned}
\tau_{rr|r=a} &= 2\sigma_0 \sum_{n=0}^{\infty} (\varepsilon_n i^{n-1}/m_n^0)\{n-h_n(\beta a)\}\cos n\theta\, e^{-i\omega t},\\
\tau_{\theta\theta|r=a} &= (1-2/k^2)\tau_{rr|r=a},\\
\tau_{r\theta|r=a} &= -4\sigma_0 \sum_{n=1}^{\infty} (ni^{n-1}/m_n)\sin n\theta\, e^{-i\omega t},\\
\mu_{rz|r=a} &= 0.
\end{aligned} \tag{52}$$

Static solution. Long wavelength approximation

The static solution, the zero-frequency limit of the dynamic solution, goes singular in both the couple-stress and the classical theories in the present case. The singularity arises out of the $n = 1$ terms in equations (51) which tend to infinity as $\omega \to 0$. The principal forms of the $n = 1$ terms at small frequencies obtained from the use of approximations (37) and (38) are

$$\begin{aligned}
\tau^{(1)}_{rr|r=a} &\sim Z\cos\theta, & \tau^{(1)}_{\theta\theta|r=a} &= (1-2/k^2)\tau^{(1)}_{rr|r=a},\\
\tau^{(1)}_{r\theta|r=a} &\sim -Z\sin\theta, & \mu^{(1)}_{rz} &\sim 2(l^2/a)k_1(a/l)Z\sin\theta,
\end{aligned} \tag{53}$$

where the superscript (1) is used as a label reference to the source of these terms and

$$Z = 2i\sigma_0/[(1+k^2)\alpha a \ln(\alpha a)]. \tag{54}$$

The first three of the asymptotic forms (53) do not depend upon the parametric length l and, therefore, also represent the principal forms of the $n = 1$ terms in equations (52).† As $l \to 0$,

† The asymptotic expressions (53) differ from the ones given in [13] which seem to be in error.

by equation (39), $l^2k_1(a/l) \to 0$ and, consistent with the last of equations (52), $\mu_{rz}^{(1)} \to 0$. The other terms in equations (51) and (52) being the same as in equations (45) and (47), approach their usual limits displayed through equations (48) and (50).

The static solution in either theory, being independent of the density of the inclusion (see [6, 7, 12]), should be one and the same for both the finitely dense and the infinitely dense cylinders. A satisfactory explanation of the infinite stresses (53) still remains wanting in literature. One possible explanation of this singular behavior is offered by the following reason.

Small frequency approximation of the displacement of a finitely dense cylinder (Appendix) shows that while the real part of the displacement vanishes in the limit, its imaginary part tends to infinity. Holding the cylinder fixed in space requires the annihilation of the latter component of the displacement which calls for an infinite amount of energy which in turn would generate infinite stresses at the surface of the cylinder. Since only the $n = 1$ terms contribute to the force on the cylinder, the infinite surface stresses manifest themselves through these terms.

It may be noted in passing that there is no translation of the cylinder in the present case (see Appendix) and the usual static boundary conditions are again recovered.

5. NUMERICAL RESULTS

The force–stress tensor in couple-stress theory is asymmetric and thus a stress state in general cannot be reduced to a principal stress state. Accordingly, a stress concentration factor defined as the greatest local stress produced, unlike in the classical theory, does not lend itself to a simple interpretation in couple-stress theory. The numerical work here presents the redistribution of the (modified) stresses at the discontinuity surface and explores the effect of couple-stress on the classical stress distribution and concentration factors. Suited to this objective, the surface stresses will be normalized by taking $\sigma_0 = 1$. The normalized stresses will simply be called stresses, for convenience, in the sequel.

Inspection of equations (29), (45), and (51) shows that the modified boundary stresses are complex functions of the parameters: θ, ν, αa, a/l and also of s if the discontinuity is a cylinder. If one writes† a typical stress τ in its polar form

$$\tau = \tau^*(\theta, \nu, \alpha a, a/l, (s))\, e^{-i\omega t} = |\tau^*|\, e^{-i(\omega t - \varepsilon)},$$

where $|\tau^*|$ denotes the absolute value of the stress and ε = phase τ^*, then it follows that the absolute value of the stress at a particular station occurs at time $t = \varepsilon/\omega$. Because of the dependence of the phase τ^* on the polar angle θ, the absolute value, for the given values of the other parameters, is attained at different locations at different times. The absolute value of a stress affords a convenient measure of the stress distribution and would be so adopted here.

The surface stresses at a given location, as stated above, depend parametrically on the values of ν, αa, a/l and (s). Since the effect of Poisson's ratio on the stress distribution is of secondary concern here, it (ν) is fixed at 0·25 in the present work. And, for a similar reason again, s is restricted to values 1, 2 and ∞. Next, as remarked earlier, the infinite series representation of the stresses is valid only at finite frequencies. The rate of convergence of these series is fast at small frequencies. Accordingly, the nondimensional wave number αa is

† The symbol (s) is to be understood here to mean dependence on s where relevant.

let range from 0 to 4·5, this range presenting a broad spectrum of large incident wavelengths. Lastly, in accordance with the notation made by Mindlin [5, p. 6] the lower limit of the range of the radius–material characteristic length ratio, a/l, is restricted to one.

For given values of the parameters, the stresses at a particular station are obtained by summing up the real and imaginary parts of the associated infinite series and then acquiring the absolute value of the resulting complex number. This was accomplished on Burroughs B5500, the series being truncated when the absolute value of the last significant term was less than 10^{-5}. Since the stresses are either symmetrical or antisymmetrical about x-axis, the variation of stresses against the polar angle are displayed only for $0 \leq \theta \leq \pi$.

Cavity

The variation of the absolute values of the modified surface stresses $\tau^*_{\theta\theta}$ and $\tau^*_{\theta r}$ vs. θ for $a/l = 3$, and $\alpha a = 0{\cdot}25$ and 4, computed from the first two of equations (29) are shown in Figs. 2 and 3, respectively. The modified $|\tau^*_{\theta\theta}|$ stresses at the critical locations $\theta = 0$,

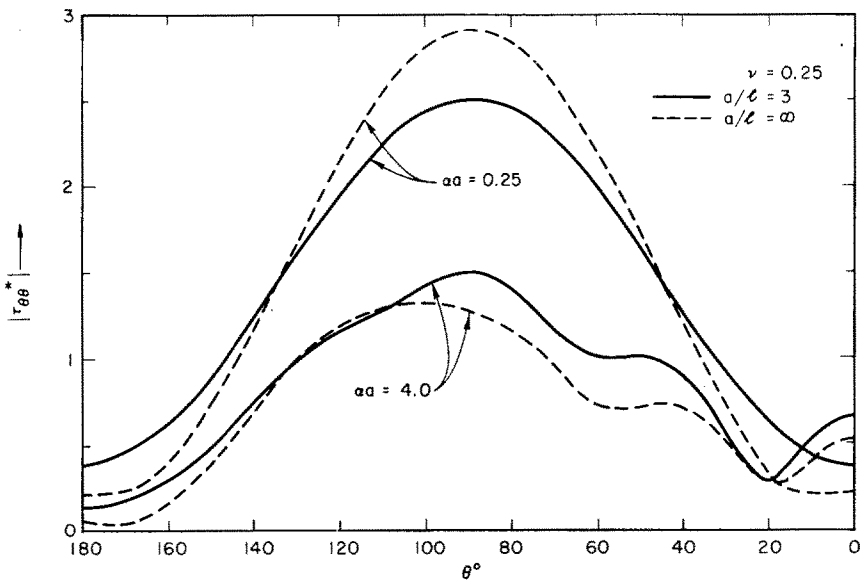

FIG. 2. Effect of couple-stresses on distribution of normalized stress $|\tau^*_{\theta\theta}|$ at a circular cavity.

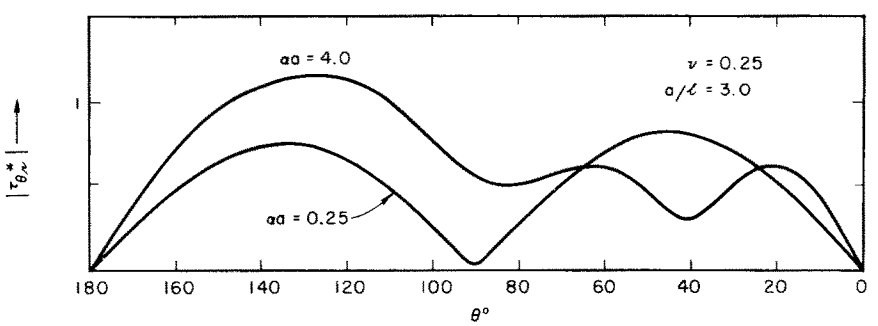

FIG. 3. Distribution of normalized stress $|\tau^*_{\theta r}|$ at a circular cavity.

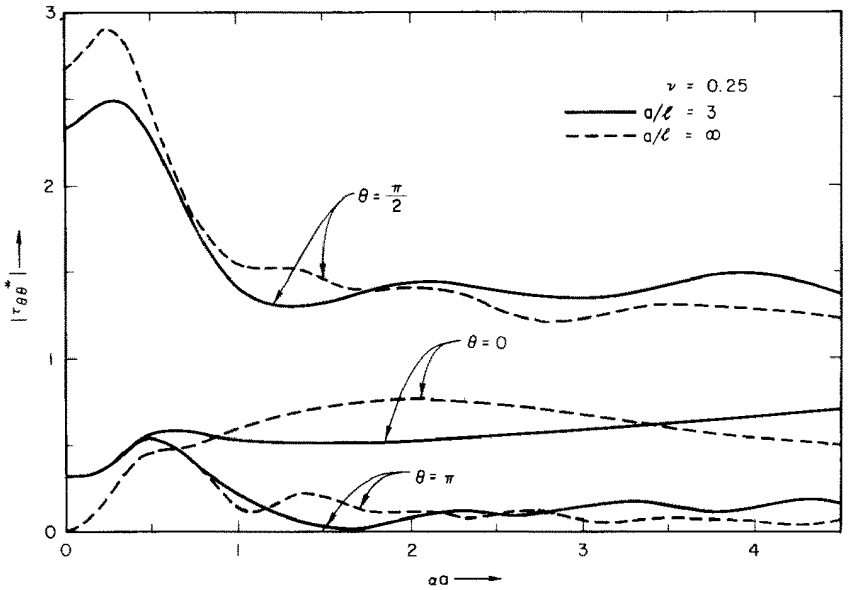

FIG. 4. Effect of couple-stresses on normalized stress $|\tau^*_{\theta\theta}|$ at locations $\theta = 0$, $\pi/2$ and π of a circular cavity vs. wave number.

$\pi/2$ and π of the cavity for varying αa and $a/l = 3$ are displayed in Fig. 4. Corresponding curves for the classical case, $a/l = \infty$, obtained from the first of equations (32) are also presented in these figures for comparison. One sees in Figs. 2 and 3 that the absolute stress distribution is nearly symmetric about $\theta = \pi/2$ for $\alpha a = 0{\cdot}25$ and not symmetric for $\alpha a = 4{\cdot}0$. This is to be expected since the zero frequency, static limit is symmetric. The figures show that the modified stresses at certain wavelengths appreciably differ from their classical values. Figs. 2 and 3 display the relative importance of the hoop stress $\tau_{\theta\theta}$ compared to the shearing stress $\tau_{\theta r}$. From Figs. 2 and 4, it is seen that the modified peak value of $|\tau^*_{\theta\theta}|_{r=a}$ at a given wave number αa occurs, as in the classical case, at around $\theta = \pi/2$, the top peak value occurring at about $\alpha a = 0{\cdot}25$. Although not a principal stress, the modified peak values of $\tau^*_{\theta\theta}$ provide a convenient measure of dynamic stress concentration factors in the modified theory. The modified dynamic factors thus defined for $\alpha a = 0{\cdot}25$, $1{\cdot}5$ and $4{\cdot}0$ and varying a/l are plotted in Fig. 5, wherein for comparison purposes, the corresponding static curve, $\alpha a = 0$, obtained from the first of equations (34) and (36) is also displayed. Figs. 4 and 5 show that the modified dynamic factors unlike their static counterpart may, depending upon the size of the incident wavelength, be greater or smaller than their corresponding classical dynamic values. The results show that for $\nu = 0{\cdot}25$ and $a/l = 3{\cdot}0$, the modified dynamic factors at $\alpha a = 0{\cdot}25$ and $4{\cdot}0$ are, respectively, 13·4 per cent less and 17·3 per cent greater than the corresponding classical dynamic factors. To compare the dynamic deviations against the static one, the static modified factor for the uniaxial strain case at $a/l = 3$, Figs. 4 and 5, is 12·4 per cent less than its corresponding classical static value.

Rigid cylinder

Inspection of the second of equations (45) and its analogs in the limiting special cases shows that at the cylindrical surface $|\tau^*_{\theta\theta}| < |\tau^*_{rr}|$. Accordingly, the distribution of stresses

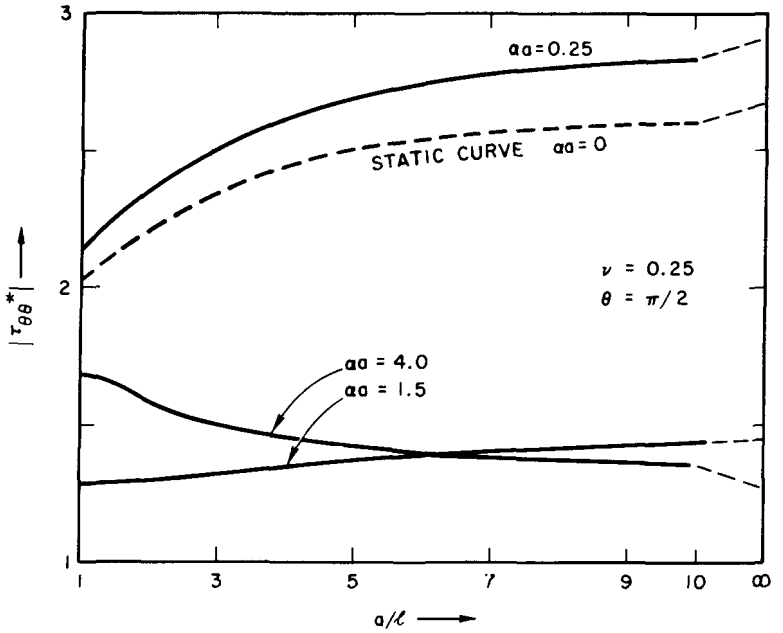

FIG. 5. Modified dynamic stress concentration factors at a circular cavity in a field of uniaxial strain.

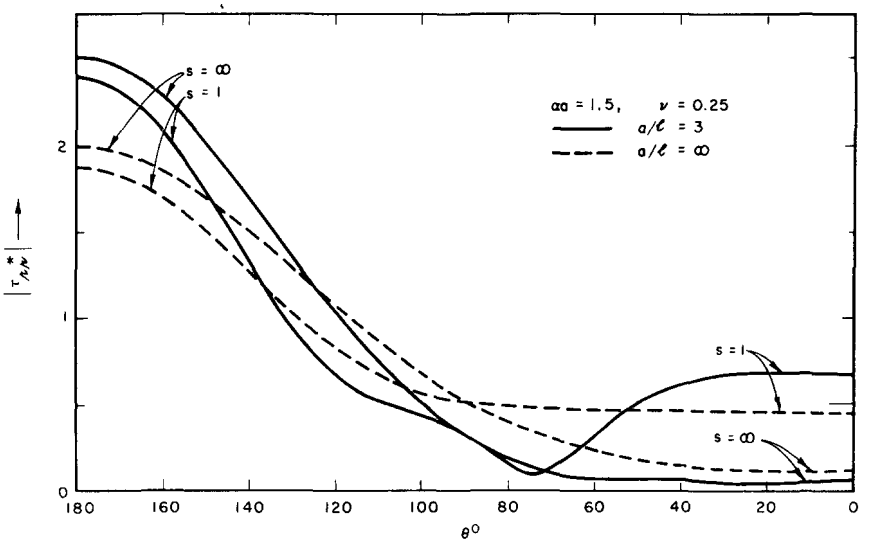

FIG. 6. Effect of couple-stresses on distribution of normalized stress $|\tau^*_{rr}|$ at a rigid circular cylinder.

τ^*_{rr} and $\tau^*_{r\theta}$ only will be considered here. Fig. 6 shows the plot of $|\tau^*_{rr}|$ at $r = a$ vs. θ for $\alpha a = 1{\cdot}5$, and $(s, a/l) = (1, 3), (1, \infty), (\infty, 3), (\infty, \infty)$, respectively, computed from the first of equations (45), (46), (51) and (52). The figure suggests that for a given wave number, the modified peak values of $|\tau^*_{rr}|$ occur, as in the classical case, at $\theta = \pi$. For the above $(s, a/l)$

pairs, curves for critical locations $\theta = 0$ and π and varying αa, the pertinent static values computed from the first of equations (48) and (50), are presented in Fig. 7. The curves show that the modified results especially the ones for $\theta = \pi$ greatly differ from the classical results.

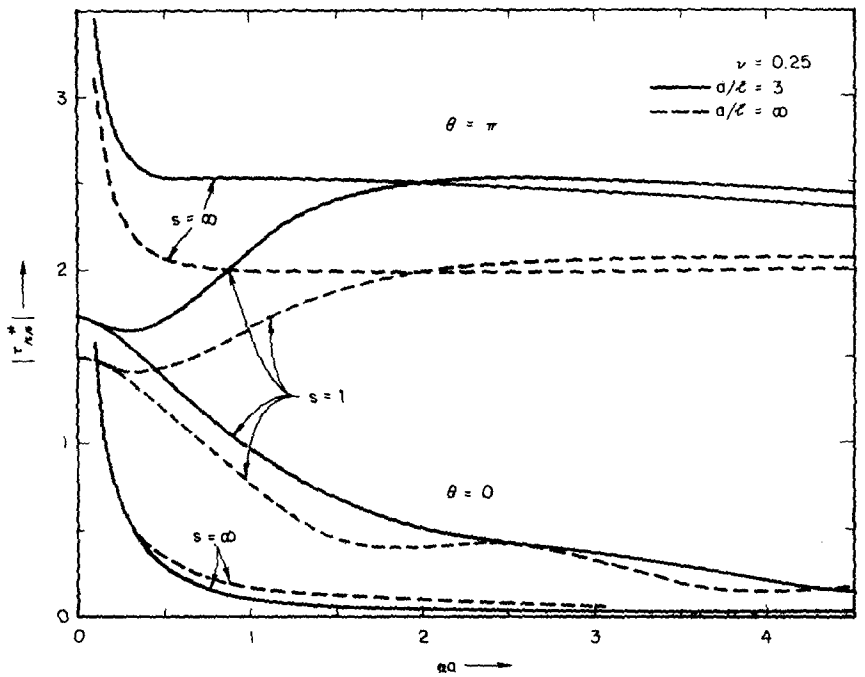

FIG. 7. Effect of couple-stresses on normalized stress $|\tau^*_{rr}|$ at locations $\theta = 0$ and π of a rigid circular cylinder vs. wave number.

For the stated values of the parameters the absolute values of $\tau^*_{r\theta}$ for varying θ, obtained from the third equations of (45), (46), (51) and (52) are plotted in Fig. 8. As shown in this plot the stress $\tau^*_{r\theta}$ vanishes at $\theta = 0$ and π. Simple algebra shows that the modified stress

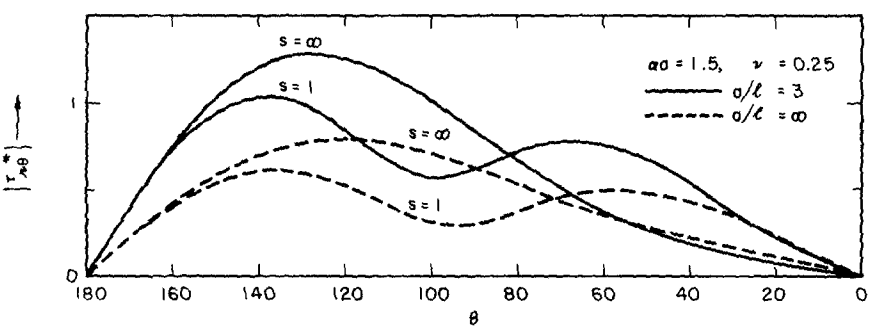

FIG. 8. Effect of couple-stresses on distribution of normalized stress $|\tau^*_{r\theta}|$ at a rigid circular cylinder.

$\tau^*_{\theta r}$ also vanishes at these locations. Accordingly, for given values of s, a/l and αa, the modified stress $|\tau^*_{rr}|_{r=a}$ at $\theta = \pi$ represents the dynamic stress concentration factor for a cylinder in the modified theory. The effect of couple-stresses on dynamic stress concentration

factors for $s = 1, 2$, and ∞, and $\alpha a = 1{\cdot}5$ is displayed in Fig. 9 wherein, for comparison, the corresponding static curve is also plotted. Figs. 7 and 9 show that, for the range of αa

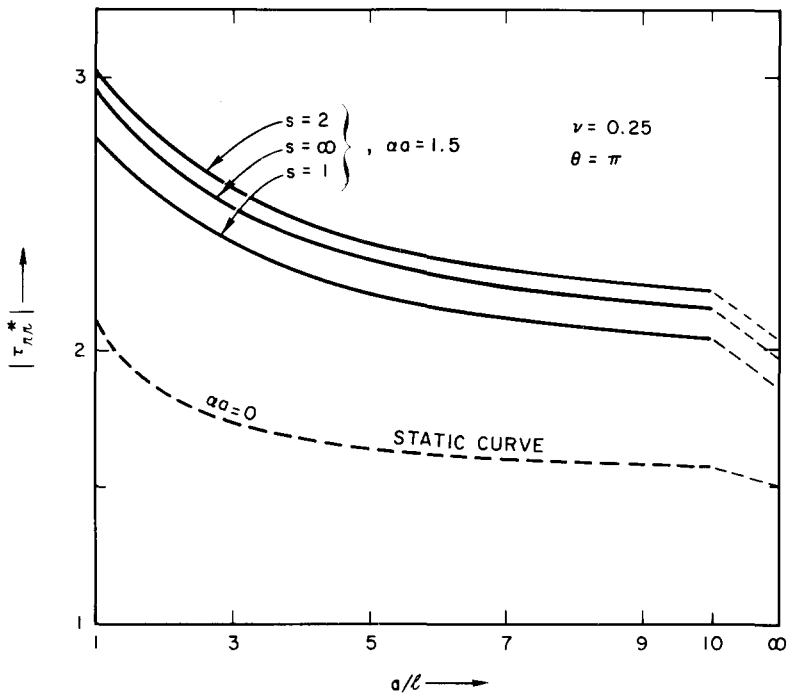

FIG. 9. Modified dynamic stress concentration factors at a rigid circular cylinder in a field of uniaxial strain.

considered, the modified dynamic factors, as in the static case, are always greater than their classical counterparts. For $\nu = 0{\cdot}25$ and $a/l = 3{\cdot}0$ the modified dynamic factor at $\alpha a = 1{\cdot}5$ is, for different densities of the cylinder, about 27 to 28 per cent larger than its classical dynamic factor. Compared to this, the static modified factor at $a/l = 3$, Figs. 7 and 9, is 16 per cent greater than its classical static value.

Acknowledgement—The authors express their appreciatiation to Mr. Vahe Sagherian of the Stanford Research Institute for programming the numerical results presented here.

REFERENCES

[1] R. D. MINDLIN and H. F. TIERSTEN, Effects of couple-stresses in linear elasticity. *Archs ration. Mech. Analysis* **11**, 415 (1962).
[2] R. MUKI and E. STERNBERG, The influence of couple-stresses on singular stress concentrations in elastic solids. *Z. angew. Math. Phys.* **16**, 616 (1965).
[3] A. E. GREEN and W. ZERNA, *Theoretical Elasticity*, p. 39. Oxford University Press (1960).
[4] K. F. GRAFF and Y. H. PAO, The effect of couple-stresses on scattering of plane waves by a spherical cavity, *Proc. 10th mid-west. Mech. Conf.*, Fort Collins, Colorado (1967). To appear.
[5] R. D. MINDLIN, Influence of couple-stresses on stress concentrations. *Exp. Mech.* **3**, 1 (1963).
[6] Y. WEITSMAN, Couple-stress effects on stress concentration around a cylindrical inclusion in a field of uniaxial tension. *J. appl. Mech.* **32**, 424 (1965).

[7] R. J. HARTRANFT and G. C. SIH, The effect of couple-stresses on the stress concentration of a circular inclusion. *J. appl. Mech.* **32**, 429 (1965).
[8] F. G. FRIEDLANDER, Diffraction of pulses by a circular cylinder. *Communs pure appl. Math.* **7**, 705 (1954).
[9] B. R. LEVY and J. B. KELLER, Diffraction by a smooth object. *Communs pure appl. Math.* **12**, 195–201 (1959).
[10] N. W. MCLACHLAN, *Bessel Functions for Engineers*, pp. 190–206, 2nd edition. Oxford University Press (1955).
[11] Y. H. PAO, Dynamical stress concentration in an elastic plate. *J. appl. Mech.* **29**, 299 (1962).
[12] J. N. GOODIER, Concentration of stress around spherical and cylindrical inclusions and flaws. *Trans. Am. Soc. mech. Engrs* **55**, 43–44 (1933).
[13] Y. H. PAO and C. C. MOW, Dynamic stress concentration in an elastic plate with rigid circular inclusion. *Proc. 4th U.S. natn. Congr. appl. Mech.* 335 (1962).
[14] J. W. MILES, Motion of a rigid cylinder due to a plane elastic wave. *J. acoust. Soc. Am.* **32**, 1656 (1960).

APPENDIX

Motion of rigid cylinder

From equations (43) and (42) one obtains the displacement U of a finitely dense rigid cylinder in a couple-stress medium in normalized form as

$$\frac{U}{\alpha\varphi_0} = \frac{4}{\alpha am}[1+\gamma^2+x_1]\,e^{-i\omega t}, \tag{55}$$

where $\alpha\varphi_0$ is the displacement-amplitude of the incident wave. Equation (55) simplifies in the special case $s = 1$ and may with the use of the recurrence relation

$$2H_1(z) = z[H_0(z)+H_2(z)],$$

be written as

$$\frac{U}{\alpha\varphi_0} = \frac{4}{\pi(\alpha a)^2 H_2(\alpha a)}\,e^{-i\omega t}. \tag{56}$$

The motion in this case, being independent of β, β_1 and β_2, is similar to one in an acoustic medium.

Use of equations (37) and (38) in equation (55) gives motion at large wavelengths as

$$\frac{U}{\alpha\varphi_0} = i[1+0(\omega^2 \ln \omega)]\,e^{-i\omega t} \tag{57}$$

so that at zero frequency, U tends to infinity through purely imaginary values, asymptotically given as $U \sim i\alpha\varphi_0$.

At high frequencies–short wavelengths, the equations defining β_1, β_2 and γ^2 approximately become

$$\beta_1, \beta_2 = \sqrt{\beta/l}[1+0(1/\omega)], \qquad \gamma^2 = 1+0(1/\omega). \tag{58}$$

The large argument approximations of the quotient functions $h_1(z)$ and $k_1(z)$, equations (26), from the use of the asymptotic expansions for large arguments of the pertinent Bessel functions [10, item Nos. 130 and 204] are obtained as

$$\begin{aligned} h_1(z) &= iz\left[1-\frac{i}{2z}+0\left(\frac{1}{z^2}\right)\right], \\ k_1(z) &= z\left[1-\frac{1}{2z}+0\left(\frac{1}{z^2}\right)\right]. \end{aligned} \tag{59}$$

With the application of equations (58) and (59) and the use of the asymptotic expansion of $H_1(z)$ for large z, equation (55) gives the motion of the cylinder at high frequencies as †

$$\frac{U}{\alpha\varphi_0} = -\frac{1}{s\pi^{\frac{1}{2}}}\left(\frac{2}{\alpha a}\right)^{\frac{1}{2}}\left[1+0\left(\frac{1}{\omega^{\frac{1}{2}}}\right)\right]\exp[-i(\alpha a+\omega t-\pi/4)]. \tag{60}$$

In the limiting case, $l \to 0$, equation (55) with the use of approximations (37) and (39), give the motion of the cylinder in the classical medium as

$$\frac{U}{\alpha\varphi_0} = \frac{4[2-h_1(\beta a)]}{\alpha a m^0}\,e^{-i\omega t}, \tag{61}$$

which agrees with the corresponding expression previously given by Miles [14]. The long and short wavelengths approximations for this special case are again given by equations (57) and (60), respectively, where now the second and higher order terms do not contain the parameter l.

In case of an infinitely dense cylinder, s is infinite and from equation (44), $\delta \sim s\delta_1$, $m \sim s\pi H_1(\alpha a)\delta_1$, and equation (55), in the limit $s \to \infty$, gives

$$U = 0. \tag{62}$$

The absolute value of the normalized displacement $|u^*| = |U/\rho\varphi_0|$ for varying a/l is plotted in Fig. 10 for $\nu = 0{\cdot}25$, $s = 1{\cdot}0$ and $2{\cdot}0$, and $\alpha a = 0{\cdot}25$, $1{\cdot}0$ and $2{\cdot}0$. The results

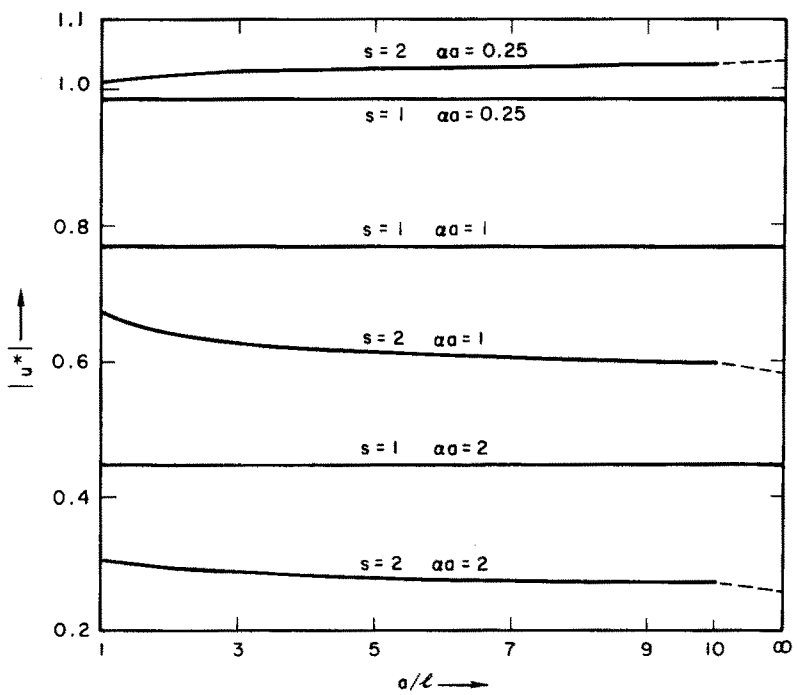

FIG. 10. Motion of a rigid finitely dense circular cylinder in a field of uniaxial strain in couple-stress medium. $\nu = 0{\cdot}25$.

† The material characteristic length l does not affect the principal term.

show that for $s = 2$, the couple-stress value of $|u^*|$, depending upon the wavelength, may be less or greater than its corresponding classical value. For $s = 2$ and $a/l = 3$, there is an increase of 7·2 per cent for $\alpha a = 1{\cdot}0$ and of 10·7 per cent for $\alpha a = 2{\cdot}0$.

(*Received* 29 *May* 1968; *revised* 23 *September* 1968)

Абстракт—Исследование касается эффекта моментных напряжений на поведение динамических напряжений, возникших вокруг круглой, цилиндрической инклюзии, находящейся в бесконечной среде, вследствие дифракции посоянных, плоских, параллельных, упругих волн сжатия, распространяющихся в среде. Исследуются полость и жесткий цилиндр с неподвижним цилиндром, рассматриваемым в качестве специального случая этого последнего. Приводятся, в виде кривых, численные результаты, важные при больших длинах волн, дл я установленного коэффициента Пуассона, которые указывают изменение модифицированных напряжений по отношению к разным параметрам. Они сравниваются с классическими значениями, полученными в качестве предельного случая. В любом случае, при некоторых длинах волн, появляются хорошо заметные отклонения от классических результатов. Обсуждается эффект моментных напряжений на движение жесткого цилиндра.